JJMIE

Volume 18, Number 4, December. 2024
ISSN 1995-6665
Pages 835- 845
https://doi.org/10.59038/jjmie/180415
Editor-in-Chief: Prof. Ali M. Jawarneh

Jordan Journal of Mechanical and Industrial Engineering

Numerical Simulations of Flow and Flame Characteristics of Double Cavity Trapped Vortex Combustor

Kousik Kumaar. R[1*], Jini Raj. R[1], Srikanth H V[3], M. Kesavan[2]

[1]Assistant Professor, Department of Aeronautical Engineering, Nitte Meenakshi Institute of Technology, Bengaluru, India
[2]Assistant Professor, Department of Aeronautical Engineering, Nehru Institute of Engineering and Technology, Coimbatore, India
[3]Professor and Head, Department of Aeronautical Engineering, Nitte Meenakshi Institute of Technology, Bengaluru, India

Received 16 Jul 2024 *Accepted 17 Oct 2024*

Abstract

This study utilizes numerical simulations to investigate combustion efficiency in a Double Cavity Trapped Vortex Combustor (DCTVC). The DCTVC, employing a double cavity design and a cavity stabilization concept, enhances flame stability and minimizes pressure drop, achieving optimal performance by injecting an appropriate mix of fuel and air into the first cavity. Vortices and eddies are utilized to achieve the greatest turbulent mixing in the DCTVC combustion chamber. Because turbulence is precisely contained inside the two chambers where reactants are introduced and effectively blended, this enhances the efficiency of the fuel and air blending process. The momentum flux ratio between the cavities and mainstream flow significantly impacts the flow structure in the cavity region under under-reacting flow circumstances. Studying NO_x emissions in combustors is imperative due to their relationship with turbulence intensity, recirculation zones, and trapped vortex zones, which directly impact combustion efficiency and emission levels. Staged combustion systems, commonly associated with DCTVCs, exhibit the potential for a substantial 30% to 60% reduction in NO_x emissions. A parametric study, varying parameter such as the cavity's geometry provides valuable insights in flow and flame structure, demonstrating the adaptability and efficiency of combustion in the DCTVC.

Keywords: DCTVC, Combustion Efficiency, Fuel-air blending, NOx emission, Flame Stabilization.

1. Introduction

Recent advancements in gas turbine engine combustion chambers have focused on using trapped vortex designs to enhance combustion efficiency and stability. Trapped vortex design incorporates cavities that capture and stabilize vortices, providing enhanced flame stabilization and reducing harmful emissions like nitrogen oxides (NO_x). One notable innovation in trapped vortex system is the Double Cavity Trapped Vortex Combustor (DCTVC), which features both a primary cavity zone and an auxiliary cavity zone. Accurate fuel mixing with the right amount of air is crucial to create a stoichiometric mixture in the primary zone, where most of the fuel burning takes place [1-2]. Before the mixture reaches the turbine, it is cooled in the secondary zone by the combination of unburned air and combustion products. An intermediate zone, which helps the secondary zone burn out soot and remove dissociation products, may be included in some designs [3-5]. Ensuring stable combustion despite high air flow rates is crucial, and the TVC achieves this through meticulous design considerations that optimize air-fuel mixing, ignition, and subsequent combustion with additional air [6-9].

The balance that exists between NO_x and CO/UHC production has complicated efforts to lower NO_x emissions in conventional combustors [10-11]. Developed with these factors in consideration, the DCTVC is a promising concept that aims to minimize NO_x emissions and enhance combustion efficiency. The unique design incorporates two cavities and employs vortex trapping principles for enhanced flame stabilization and combustion efficiency [12]. This design aligns with the Rich Quench Lean strategy, a staged combustion process known to lower emissions.

A distinctive feature of the DCTVC is that combustion processes may extend downstream when unburned gases mix with the mainstream oxidizer, representing a staged combustion process [13]. This approach addresses challenges related to removing the mixture of unburned gases from the combustion chamber and mitigating nitric oxide formation [14-15]. Lean premixed combustion introduces an alternative concept to reduce nitric oxide emissions for power generation.

The studies on combustor chambers investigated the hydrodynamics and separation efficiency of vortex separators using computational fluid dynamics (CFD) and advanced turbulence modelling, focusing on the Reynolds Stress Model (RSM) [16-17]. The researchers aimed to

* Corresponding author e-mail: kousikkumaarphd@gmail.com.

  - Volume 18, Number 4 (ISSN 1995-6665)

optimize double vortex cylindrical separators for multiphase flows, such as air-water and solid particle separation. Vortex generators enhanced separation efficiency by directing different phases to specific regions within the separator [18]. The analysis demonstrated that higher swirl numbers lead to increased pressure drops, tangential velocities, and contraction of vortex cores. Numerical simulations, validated by experimental data and large eddy simulation (LES), accurately predicted flow patterns, with RSM outperforming models like k-epsilon in capturing complex swirling behaviours [19]. The study examined the role of radial pressure gradients and axial velocity transitions on vortex stability, noting challenges in modelling free-to-forced vortex transitions [20]. The findings are relevant for optimizing industrial separators, gas turbines, and combustion systems, and suggest future research on varied geometries, particle characteristics, and flow conditions for enhanced design [21].

The combustor chamber research highlighted various emission challenges associated with different fuel types and combustion methods. In syngas combustion using a lean premixed swirl-stabilized burner, both NO_x and CO emissions increased as the global equivalence ratio decreased, although syngas produced lower CO and NO_x emissions compared to natural gas and NG+H_2 mixtures [22]. In a dual-fuel engine using LPG and diesel, while NOx and smoke emissions were reduced, high hydrocarbon (HC) and carbon monoxide (CO) emissions were observed, particularly at lower loads [23]. The introduction of a glow plugs improved combustion efficiency, significantly reducing HC and CO emissions but did not affect NO_x levels. Additionally, transesterified biodiesel (sunflower methyl ester, SFME) blends demonstrated higher NOx emissions compared to conventional diesel; however, employing exhaust gas recirculation (EGR) successfully reduced NO_x emissions by approximately 25% at the same power output while increasing smoke, CO, and unburnt HC emissions [24-25].

To enhance the DCTVC design, objectives include increasing residence time while minimizing pressure drop, achieving at least 98% combustion efficiency, and lowering NO_x emissions. The priorities for improvement include lean-blow-out, durability, and altitude relight, taking into consideration weight, cost, and the temperature profile at the combustor's exit. With the aim to prevent any fraction loss, the primary objective is to ensure perfect fuel and air mixing within the two chambers.

2. Methods

2.1. Designing of Double Cavity Trapped Vortex Combustor (DCTVC)

In the numerical simulation of the double cavity trapped vortex combustor (DCTVC), six cases of combustor was taken into the consideration. The design phase was made directly in the ANSYS Workbench Design modeller. The combustor design model was developed based on the research findings of Yi Jin *et al*. [2] and analysis of the combustors were taken in 2D flow analysis conditions which would be efficient to understand the flow characteristics of each case of combustors.

When compared to a traditional swirl combustor, the single cavity trapped vortex combustor demonstrates significantly lower total pressure loss. This efficiency prompted the exploration of a double cavity trapped vortex combustor design [27]. The six models are as follows,

1. Model I – Normal combustor without secondary airflow,
2. Model II – Normal combustor with secondary airflow,
3. Model III – DCTVC with normal square cavities without secondary airflow,
4. Model IV – DCTVC with normal square cavities with secondary airflow,
5. Model V – DCTVC with Stepped square cavities without secondary airflow,
6. Model VI – DCTVC with Stepped square cavities with secondary airflow.

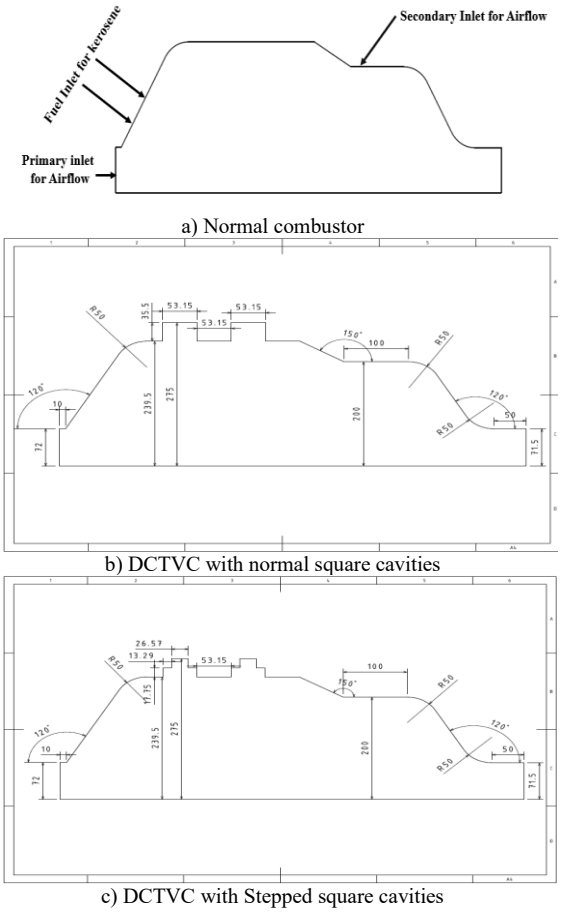

Figure 1. Combustor Models

2.2. Meshing

A structured mesh was generated for all the models to enhance the flow capturing capability and getting accurate results as shown in Fig 2 a. The model was uniformly divided into three sections and meshed to achieve an optimal meshing strategy. A grid independence study was conducted by refining the mesh into coarse, medium, and fine grids, with element sizes of 0.75 mm, 0.5 mm, and 0.25 mm, respectively. The corresponding element counts for the coarse, medium, and fine meshes were 242,755, 385,276, and 542,172. Additionally, the total pressure distribution along the combustor axis was evaluated for each mesh configuration, using a convergence criterion of 10^{-5} (Fig.

2b). The grid independence results indicated that the total pressure along the combustor axis, post-combustion, was nearly identical for the medium and fine meshes. Given the need to balance computational accuracy and efficiency, the medium mesh with structured grids was selected for further analysis. This meshing approach ensures optimal flow capture while maintaining computational feasibility. Mesh characteristics for all models are summarized in Table 1.

Table 1. Statistical Data of Mesh

	Model I	Model II	Model III	Model IV	Model V	Model VI
Nodes	387178	388116	387926	392118	387684	389444
Elements	385276	387824	385954	391496	385598	389292

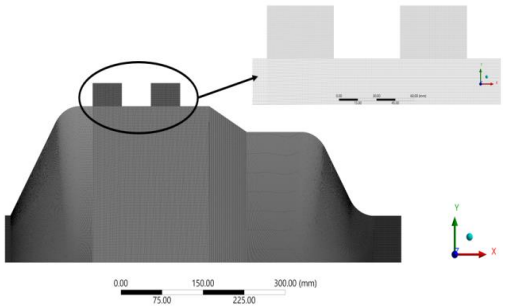

a) Fine structured mesh

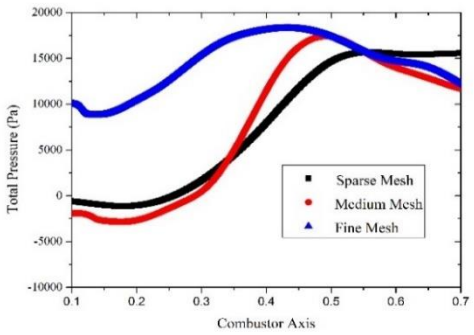

b) Grid independency test

Figure 2. Details of Meshing

2.3. Boundary Conditions

The inlet boundary conditions for the flow analysis are illustrated in the following table 2. The air medium was taken as the oxidizing medium from the compressor to combustor whereas, kerosene was taken as the fuel medium which is let through a separate fuel inlet.

Table 2. Inlet Boundary Conditions

Conditions	Air	Kerosene
Total Pressure, bar	20.68	96.50
Static Pressure, bar	20.68	-
Temperature, K	611.11	300
Velocity, m/s	121.92	152.4
Density, kg/m^3	24.02	800.92
Mass Flow rate, kg/s	29.93	1.38

2.4. Numerical Modelling

The numerical analysis used in this present work is managed by the tool ANSYS Fluent 22.0. A finite volume approach with an implicit method is employed to solve this computational framework for better stability. The steady-state analysis is processed for this numerical modelling and SST k-ω turbulence model is considered to predict the mixing characteristics inside the model. For this proposed analysis, a SIMPLE algorithm with a second-order upwind scheme is employed to quantize the governing equations for the pressure and velocity. Furthermore, the species transport model is utilised for the uniform combustion of JP-5 Kerosene- MIL-DTL-5624.

The molecular composition of the kerosene, specifically within the carbon chain range of C_{15} to C_{18} and utilising JP-5, corresponds to a molecular weight of 170. In FLUENT, the CFD code employs the chemical formula $C_{12}H_{23}$ in its computations for kerosene. Efficient combustion in stochiometric form is enabled through the supply of the proper amount of oxygen during the combustion process that helps to oxidize all the presented fuel particles, without any unburned fuel.

The balanced equation for the combustion process is

$$C_{12}H_{23} + 17.75O_2 \rightarrow 12CO_2 + 11.5H_2O \quad (1)$$

The AFR for stochiometric combustion of oxygen is 17.75 and the moles of air and kerosene for stochiometric combustion are expressed as

$$AFR = \frac{moles\ of\ air}{moles\ of\ kerosene} \quad (2)$$

The moles of air and kerosene are 1032 mol and 8mol respectively and the AFR is assumed as 127.2.

3. Results and Discussion

The results of the flow analysis for the normal combustor with and without secondary airflow, DCTVC with normal square cavities with and without secondary airflow and DCTVC with stepped square cavities with and without secondary airflow is discussed below.

3.1. Normal combustor without secondary airflow

The contours of pressure, velocity and temperature distribution are shown in the following for the normal combustor without secondary airflow which shows not much air-blending taking place, this leads to the emissions of NO_x-SO_x gases (Fig 3a, 3b and 3c). The static temperature distribution within the combustor shows that temperatures are significantly higher along the combustor axis, with combustion extending into the secondary zone (Fig. 3c). The temperature increase in the primary zone of the combustion chamber is lower compared to the secondary zone, suggesting a potential presence of unburned gases as the flow progresses into the secondary region.

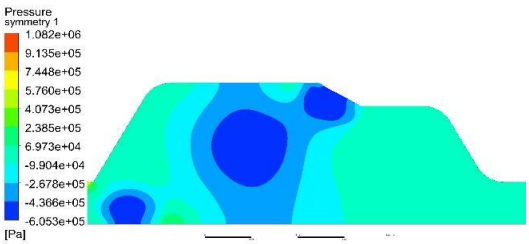

a) Pressure Distribution

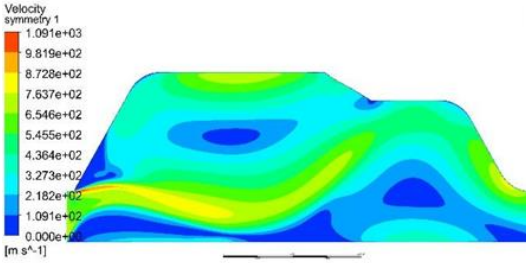

b) Velocity Distribution

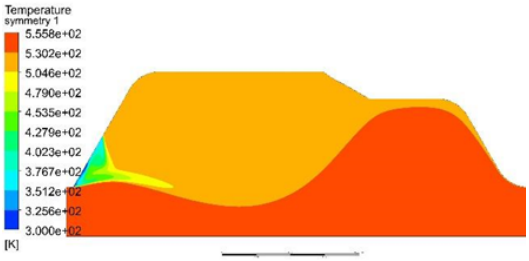

c) Temperature Distribution

Figure 3. Normal combustor without secondary airflow

3.2. Normal combustor with secondary airflow

The presented contours illustrate the distribution of pressure, velocity, and temperature for a standard combustor with secondary airflow (Fig 4a, 4b and 4c). The observed patterns suggest that there is a level of air-blending occurring, but it is below a moderate threshold, indicating a restrained blending phenomenon in the system. The injection of secondary air increases the oxygen supply, promoting the combustion of unburned fuel more effectively than in a standard combustor without secondary airflow (Fig. 4b). Additionally, the observed reduction in static temperature indicates improved mixing due to the secondary airflow, which ultimately enhances combustion efficiency (Fig. 4c).

3.3. DCTVC with normal square cavities without secondary airflow

The illustration below depicts the pressure, velocity, and temperature distribution contours for the DCTVC featuring square cavities in a standard configuration, without the presence of secondary airflow (Fig 5a, 5b and 5c). The visualization indicates a limited degree of air blending occurring in the system. In Fig. 5b, the velocity contour reveals that the cavities enhance mixing by trapping the air-fuel mixture within them. The recirculation zone generated by the DCTVC ensures that approximately 80% of the combustion takes place predominantly in the primary zone (Fig. 5c).

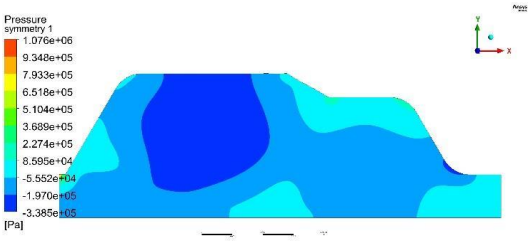

a) Pressure Distribution

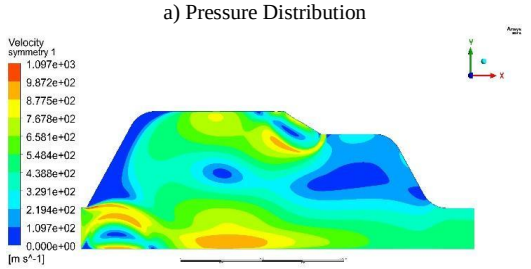

b) Velocity Distribution

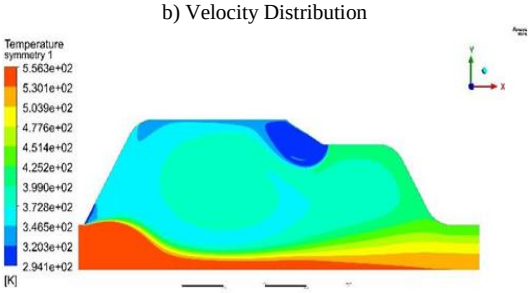

c) Temperature Distribution

Figure 4. Normal combustor with secondary airflow

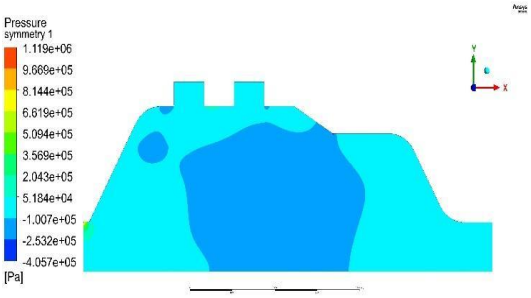

a) Pressure Distribution

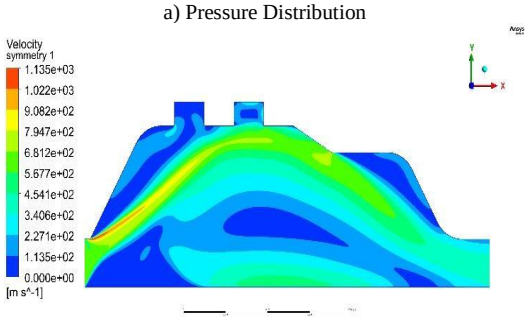

b) Velocity Distribution

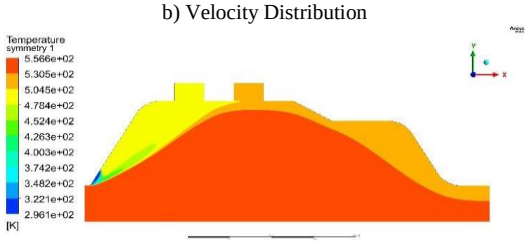

c) Temperature Distribution

Figure 5. DCTVC with normal square cavities without secondary airflow

3.4. DCTVC with normal square cavities with secondary airflow

The provided figures (6a, 6b and 6c) illustrate the distribution contours of pressure, velocity, and temperature for the DCTVC equipped with square cavities in a standard configuration, along with the inclusion of secondary airflow. The unburned gases produced during combustion are further burned with the introduction of secondary air (Fig. 6b). While the DCTVC without secondary air improves combustion through the cavities, the DCTVC with secondary airflow does not enhance combustion significantly but effectively reduces NO_x emissions. The visualization suggests a level of air-blending occurring that is at the moderate range.

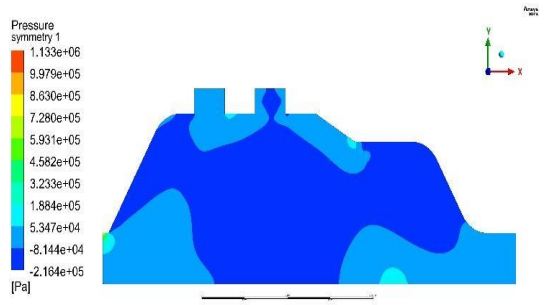

a) Pressure Distribution

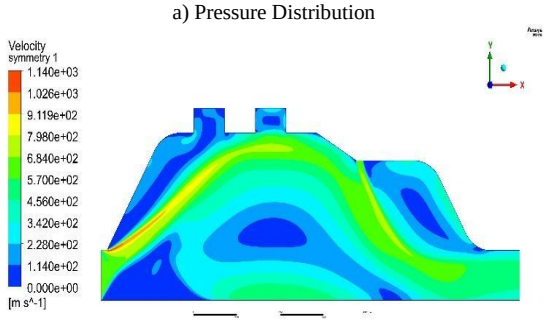

b) Velocity Distribution

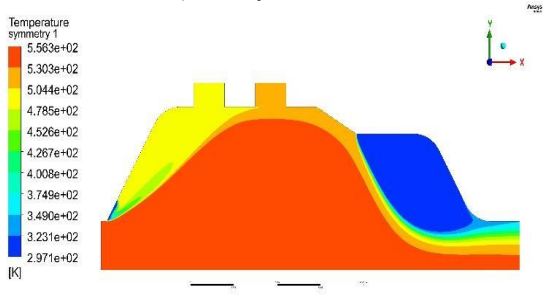

c) Temperature Distribution

Figure 6. DCTVC with normal square cavities with secondary airflow

3.5. DCTVC with Stepped square cavities without secondary airflow

The depicted contours represent the distribution of pressure, velocity, and temperature for the DCTVC incorporating stepped square cavities in a standard configuration, excluding secondary airflow (Fig 7a, 7b and 7c). The visualization indicates effective air-blending, demonstrating favourable characteristics in the system. In Fig. 7b, the velocity contour shows that the first cavity traps a greater amount of the air-fuel mixture compared to the DCTVC. This increase in the trapped mixture leads to a more uniform combustion process, which helps reduce the formation of NO_x and other harmful emissions when compared to a conventional combustor.

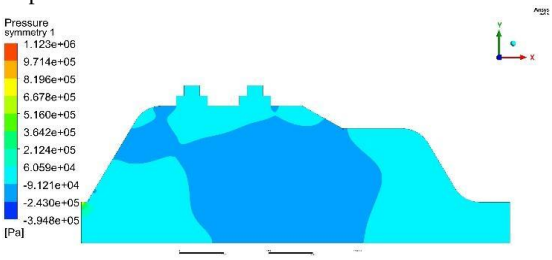

a) Pressure Distribution

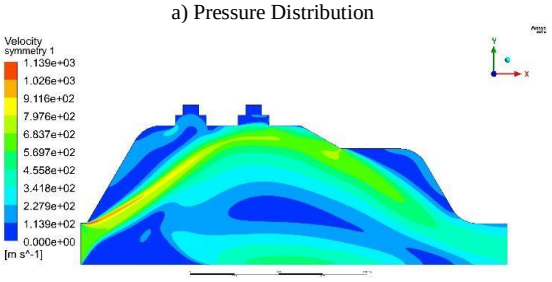

b) Velocity Distribution

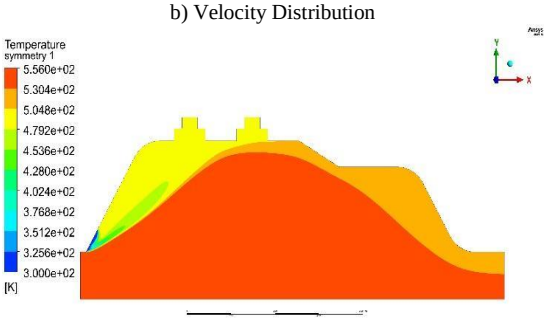

c) Temperature Distribution

Figure 7. DCTVC with Stepped square cavities without secondary airflow

3.6. DCTVC with Stepped square cavities with secondary airflow

The provided visuals display the distribution contours of pressure, velocity, and temperature for the DCTVC featuring stepped square cavities and incorporating secondary airflow. The observed patterns indicate a high level of air-blending, showcasing an excellent blending phenomenon within the system.

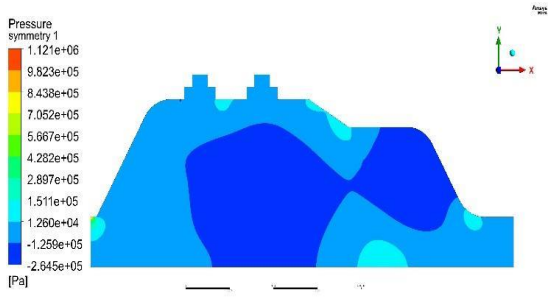

a) Pressure Distribution

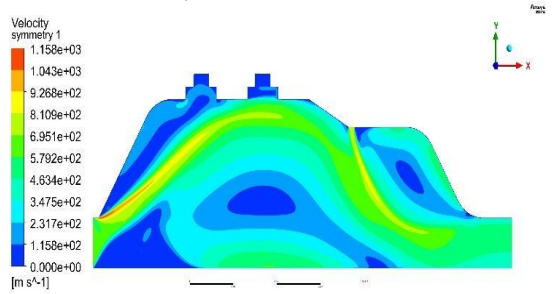

b) Velocity Distribution

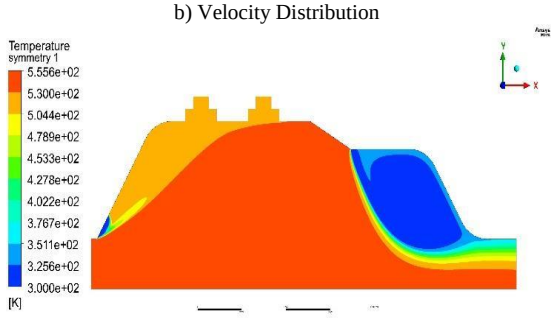

c) Temperature Distribution

Figure 8. DCTVC with Stepped square cavities with secondary airflow

Analysing the flow dynamics within the combustor models reveals that the Double Cavity Trapped Vortex Combustor, featuring Stepped Square cavities under secondary airflow conditions, exhibits superior characteristics in terms of eddy viscosity and Turbulent Kinetic Energy. This design facilitates improved blending of air and fuel compared to alternative combustor models, potentially resulting in reduced emissions of NO_x gases.

3.7. Analysis of Mixing Properties in Combustion Processes

The turbulence model used to predict the mixing properties in the combustion process is the SST k-ω turbulence model. The modelling of turbulence and species transport analysis is governed by the following basic equations.

1. Turbulent kinetic energy equation:

$$\frac{\partial}{\partial t}(\rho k)+\frac{\partial}{\partial x_j}(\rho u_j k)=\frac{\partial}{\partial x_j}[(\mu+\frac{\mu_t}{\sigma_k})\frac{\partial k}{\partial x_j}]+Q_k-\rho\varepsilon \quad (3)$$

2. Specific dissipation rate (ω) equation:

$$\frac{\partial}{\partial t}(\rho\omega)+\frac{\partial}{\partial x_j}(\rho u_j\omega)=\frac{\partial}{\partial x_j}[(\mu+\frac{\mu_t}{\sigma_\omega})\frac{\partial\omega}{\partial x_j}]+\frac{\rho\varphi}{\omega}\frac{\partial k}{\partial x_j}\frac{\partial\omega}{\partial x_j}\varsigma*\rho\omega^2 \quad (4)$$

where,

- ρ represents the density of the fluid.
- u_j represents the velocity components.
- μ represents the laminar viscosity.
- μ_t represents the turbulent viscosity.
- Q_k represents the production of turbulent kinetic energy.
- ε represents the dissipation rate of turbulent kinetic energy.
- φ and $\varsigma*$ are model constants.
- σ_k and σ_ω are model constants used for stability.

The turbulence level of the combustion process in different combustor models and the efficiency of the combustion are presented through eddy viscosity, turbulent kinetic energy and streamline contours.

3.8. Eddy Viscosity contour

The competency of the combustion process is mostly influenced by the fraternisation characteristics in the combustion chamber. Figure 9 represents the turbulent mixing characteristics of the combustion process that are endorsed due to the distribution of eddies formed. In the NC without the secondary air inlet, the eddies are formed near the primary section of the combustor (Fig 9a). The maximum amount of eddy viscosity is retained as 62.52 Pas indicating intensive mixing of fuel and air promoting the combustion reaction. However, the contour shows that mixing is largely affected downstream as the amount of eddy viscosity is decreased by about 12.5 Pas.

To enhance the complete mixing in the combustion process, the secondary air is passed into the NC. It is observed that the distribution of eddy viscosity downstream is greatly increased by the amount 87.6 Pas (Fig 9b). But still, the combustion efficiency is affected by the improper mixing of the fuel and air near the lower wall section of the combustor. Therefore, the DCTVC with a normal square cavity is introduced for the combustion process. The square cavity region because of the vacated space pulls the air upward causing the interaction of the air and fuel molecules to mix at a greater rate of about 98.5 Pas (Fig 9c).

In Figure 9d, the secondary air is passed to enhance the combustion process, enabling efficient mixing near the secondary region of the combustor. Furthermore, the combustion process of DCTVC with a stepped square cavity is presented in Fig 9e. It is observed from the reactant of combustion that the eddy viscosity rate is retained as 97.99 Pas. However, the eddy viscosity of DCTVC with stepped square and secondary air inlet is gained as 89.38 Pas. Overall, the formation of eddies indicates that the DCTVC with normal and stepped square cavities have efficient mixing characteristics due to the suction of air and fuel molecules near the square cavities.

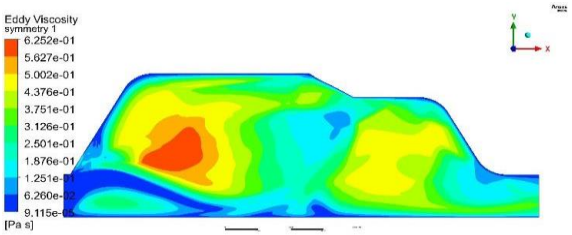

a) NC without SAI

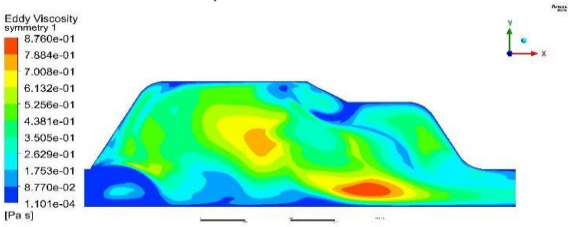

b) NC with SAI

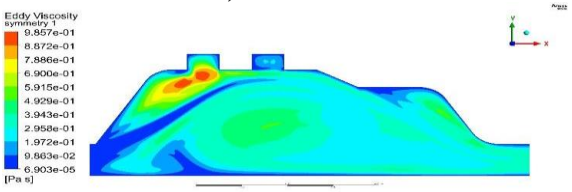

c) DCTVC with normal square cavities

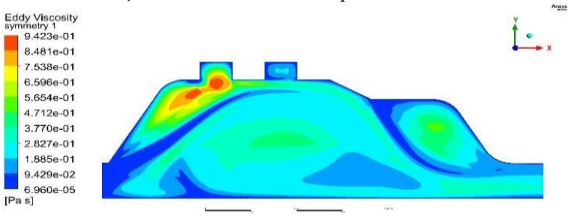

d) DCTVC with normal square cavities and SAI

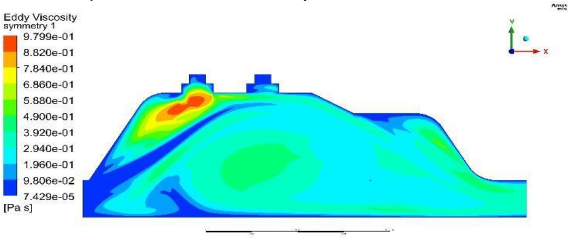

e) DCTVC with stepped square cavities

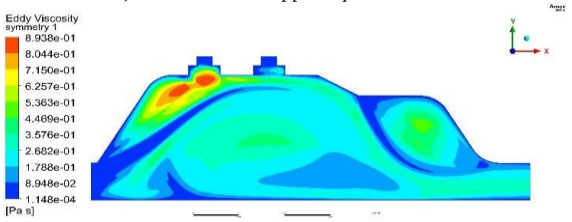

f) DCTVC with stepped square cavities and SAI

Figure 9. Eddy formation during the combustion process

3.9. Turbulent Kinetic Energy

The diffusion of the reactants in the combustion process is the main cause of the increase in TKE. In the normal combustor, the TKE created due to the fluctuation of velocity is high near the primary zone where there is a progression of diffusion of fuel and air (Fig 10a). A similar pattern is observed in the NC with SAI but there is an increase in TKE due to the amount of secondary air passed into the combustor (Fig 10b).

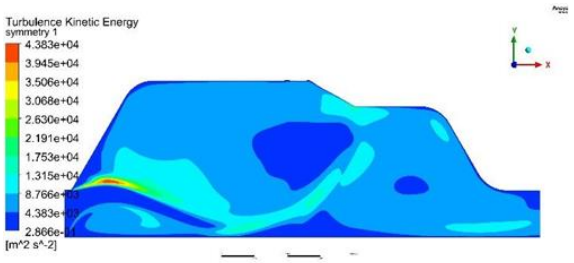

a) NC without SAI

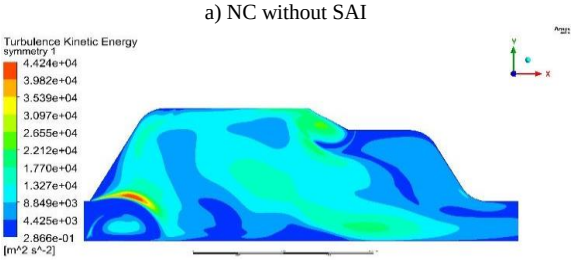

b) NC with SAI

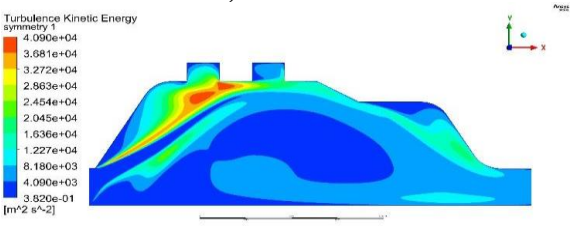

c) DCTVC with normal square cavities

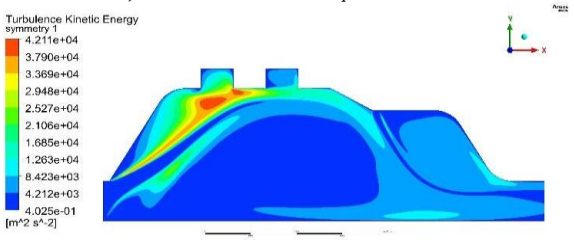

d) DCTVC with normal square cavities and SAI

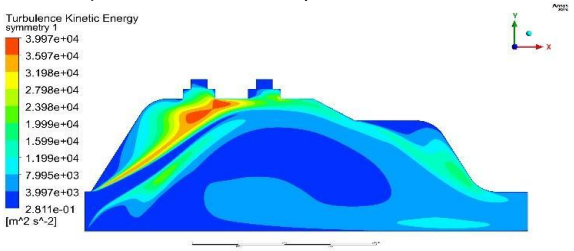

e) DCTVC with stepped square cavities

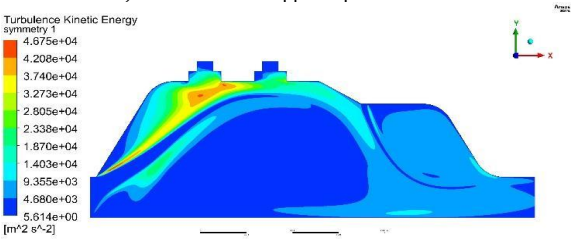

f) DCTVC with stepped square cavities and SAI

Figure 10. Turbulent K.E growth during combustion process

The distribution of eddies inside the combustor is enhanced by the DCTVC with the squared cavities. Fig 10c and 10d illustrate that there is a progressive growth in the TKE near the square cavity. This enables the recirculation region downstream which further helps in increasing the combustion efficiency because of the swirling motion

  - Volume 18, Number 4 (ISSN 1995-6665)

within the vortex chamber, the combustion byproducts remain longer time within the chamber for an extended duration, transferring heat to the surrounding walls [26]. This flow pattern guides the movement from the outer edges towards the central axis. Figures 10e and 10f show similar mixing characteristics because of the stepped square cavity which increases the TKE around it.

3.10. Vector contour plot

The flow behaviour inside the combustor can be visualized by the vectorcontours. The mixing characteristics of the combustors can be easily observed using velocity vectors. In NC, the flow pattern shows that there exists a recirculation region that promotes the mixing of the reactants in the combustion chamber as present in Fig 11a. It is also understood that the secondary air passage pulls the reactant near the upper and lower walls instigating the combustion process (Fig 11b).

The progression of square cavities improves the overall mixing of the reactants. The streamline flow patterns indicate that the diffusion process is enhanced by the normal square cavities due to the recirculation zone created by the cavities. This strengthens the mixing of the reactants largely near the primary zone of the combustor (Fig 11c). Subsequently, the secondary air passage again slows down the flow as visualized in Fig 11d. This put forth the increase in temperature distribution around the primary zone of the combustor.

Similarly, the DCTVC with a stepped square cavity combustor is checked for the same parameter. It is revealed that due to the step cut region, the diffusion occurred during combustion is improved in the primary zone increasing the overall efficiency of combustion as presented in Fig 11e and 11f. Therefore, the DCTVC with normal square and stepped square cavities augments the overall combustion as evidenced by the flow field vectors.

3.11. NO_x Emission Analysis

An analysis of NO_x emissions was conducted for both the conventional combustor model and the Double Cavity Trapped Vortex Combustor (DCTVC) with Stepped Square configuration. NO_x formation occurs because of the reaction between nitrogen and oxygen present in the combustion air at elevated flame temperatures. When flame temperatures exceed 1800 K, the high thermal energy accelerates the formation of NO_x within the combustion chamber. This thermal NO_x production is primarily driven by the Zeldovich mechanism, which becomes significant under such high-temperature conditions. Understanding, NO_x emissions in combustors is crucial due to their correlation with factors like turbulence intensity, recirculation zones, and trapped vortex zones. These elements influence combustion efficiency and emission levels, making their study essential for optimizing combustor performance, minimizing environmental impact, and ensuring regulatory compliance. The aim was to assess and comprehend the extent of NO_x gas reduction achieved with the latter in the engine.

The comparison in Table 3 between the Normal Combustor and the DCTVC with Stepped Square cavities indicates lower NO_x emissions in the latter. Specifically, at 0.6 m position, emissions were 7×10^{-2} ppm in the Normal Combustor and 5×10^{-2} ppm in the DCTVC with Stepped Square cavities. This trend is further supported by contour results (Fig 13a-b), showing reduced NO_x emissions in the DCTVC configuration compared to the normal combustor (Fig 12a-b). The improvement is attributed to enhanced air-fuel blending within the DCTVC, leading to more efficient combustion of kerosene fuel and consequently lower NO_x emissions.

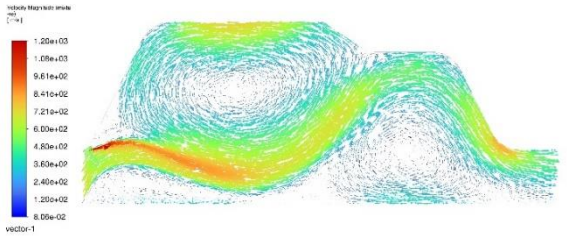

a) NC without SAI

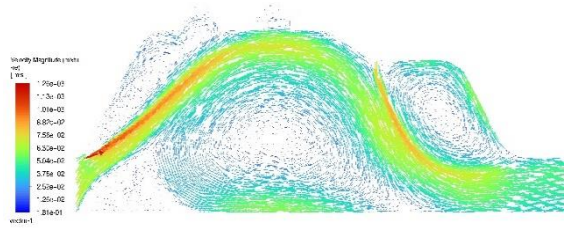

b) NC with SAI

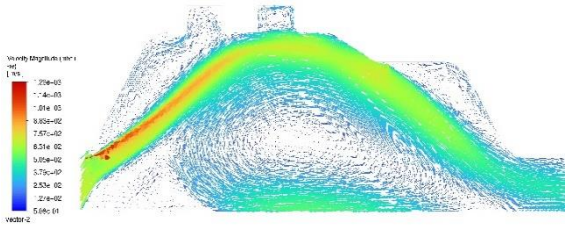

c) DCTVC with normal square cavities

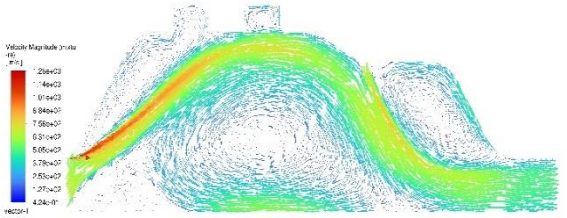

d) DCTVC with normal square cavities and SAI

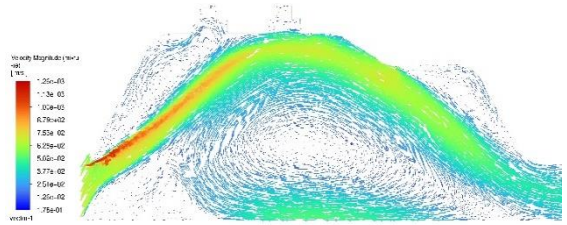

e) DCTVC with stepped square cavities

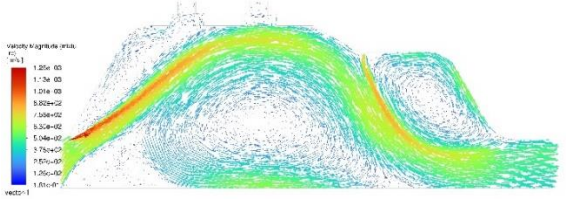

f) DCTVC with stepped square cavities and SAI

Figure 11. Flow mixing visualization through vector plots

Table 3. Comparison of NO_x emission in Normal Combustor and DCTVC with Stepped Square cavities

Type of Combustor	Position (m)	No. of Particles per Minute (PPM)	Reduction Percentage of PPM
Normal Combustor	0.6	7×10^{-2}	-
DCTVC with Stepped Square cavities	0.6	5×10^{-2}	28.57%

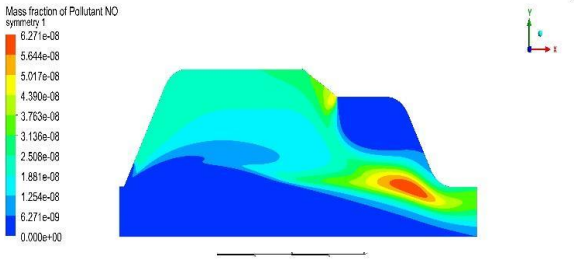

a) Contours of Pollutant NO_x Emission

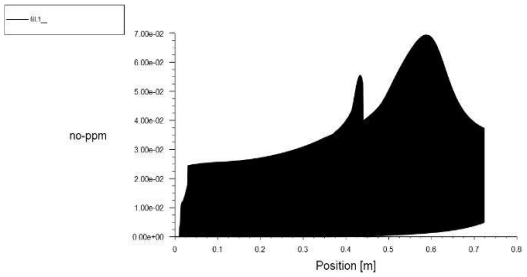

b) Position vs PPM

Figure 12. Normal Combustor Model

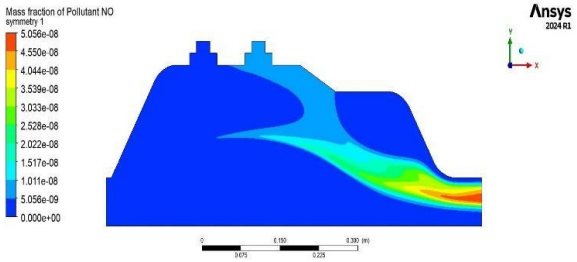

a) Contours of Pollutant NOx Emission

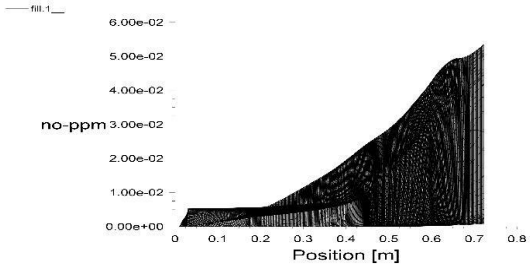

b) Position vs PPM

Figure 13. DCTVC with Stepped square cavities configuration

3.12. CO_2 Emission Analysis

The generation of CO_2 in the normal combustor and in the DCTVC with stepped square cavities is illustrated in Fig. 14(a-b). During the combustion process, CO_2 is produced in regions of the combustion chamber exposed to high temperatures. The concentration of CO_2 is directly correlated with the temperature in these zones. As shown in Fig. 15a, in the primary zone of the normal combustor, the combustion temperature exceeds 2000 K, leading to an increased concentration of CO_2. In this case, the CO_2 mass fraction reaches 0.19 and extends into the dilution region (Fig. 14a).

In contrast, the combustion temperature within the DCTVC with stepped square cavities is around 1800 K, resulting in a lower CO_2 concentration of 0.16 in the primary zone (Fig. 14b and Fig. 15b). After secondary injection, the CO_2 concentration in the normal combustor decreases to 0.09, while in the DCTVC with stepped square cavities, it drops further to 0.05 (Fig. 14a-b). The CO_2 concentration plays a critical role in combustion stability and affects the overall temperature distribution within the combustor.

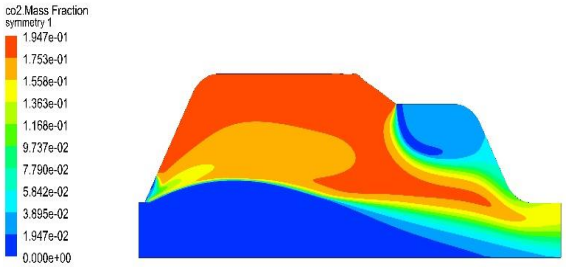

a) Normal Combustor

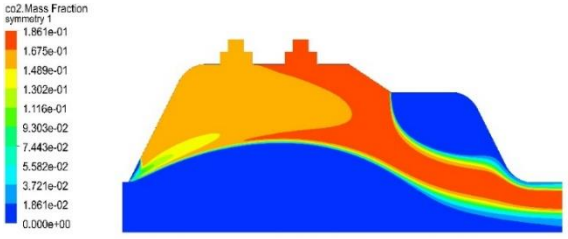

b) DCTVC with Stepped square cavities

Figure 14. Contours of Pollutant CO_2 Emission

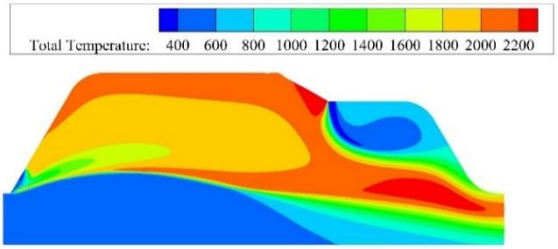

a) Normal Combustor

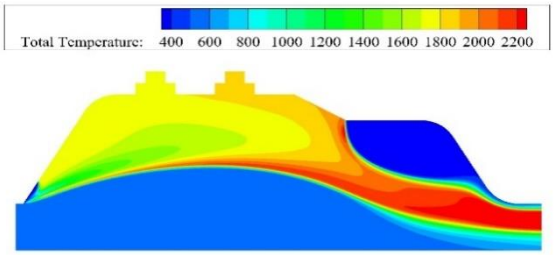

b) DCTVC with Stepped square cavities

Figure 15. Total temperature distribution contour

4. Conclusion

The investigation involved modelling combustors to analyse flow and flame characteristics. Among the six models examined, including the conventional combustor, the Double Cavity Trapped Vortex Combustor (DCTVC) with a Stepped Square cavity configuration along with secondary airflow demonstrated superior performance compared to other models. The circulation effect in the double cavity combustor has shown considerable advancement in comparison to conventional swirl combustors. Emission characteristics were assessed through numerical simulation, validating maximum flame temperature and turbine inlet temperature with a marginal error of 3.9%. As an overview of the findings, it is determined that the DCTVC with Stepped Square cavities improves flow mixing in the primary zone through enhancing flow recirculation. Implementation of this configuration in a standard engine achieved a significant 28.57% reduction in emissions.

References

[1] R. Puster, M. Egoavil, P. Gregory, D. Moslemian, "A Gas Turbine Combustor with a Double Step Combustor and a Captured Vortex Chamber", 47th AIAA Aerospace Sciences Meeting Including The New Horizons Forum and Aerospace Exposition, 5 - 8 January 2009, Orlando, Florida, AIAA 2009-1251, 2009.

[2] Yi Jin, Yefang Li, Xiaomin He, Jingyu Zhang, Bo Jiang, Zejun Wu, Yaoyu Song, "Experimental investigations on flow field and combustion characteristics of a model trapped vortex combustor", Applied Energy, Vol. 134, 2014, pp.257-269, https://doi.org/10.1016/j.apenergy.2014.08.029.

[3] Yuling Zhao, Xiaomin He, Jiankun Xiao, Mingyu Li, "Effect of cavity-air injection mode on the performance of a trapped vortex combustor", Aerospace Science and Technology, Vol. 106, 2020, https://doi.org/10.1016/j.ast.2020.106183.

[4] Zejun Wu, Yi Jin, Xiaomin He, Chong Xue, Liang Hong, "Experimental and numerical studies on a trapped vortex combustor with different struts width", Applied Thermal Engineering, Vol. 91, 2015, pp.91-104, https://doi.org/10.1016/j.applthermaleng.2015.06.068.

[5] P. K. Ezhil Kumar & D. P. Mishra, "Numerical study of reacting flow characteristics of a 2D twin cavity trapped vortex combustor", Combustion Theory and Modelling, Vol. 21, No. 4, 2017, pp. 658-676,https://doi.org/10.1080/13647830.2017.1281441

[6] K. K. Agarwal, R. V. Ravikrishna, "Experimental and Numerical Studies in a Compact Trapped Vortex Combustor: Stability Assessment and Augmentation", Combustion Science and Technology, Vol. 183, No. 12, 2011, pp.1308-1327, https://doi.org/10.1080/00102202.2011.592516

[7] Yi JIN, Xiaomin HE, Bo JIANG, Zejun WU, Guoyu DING, "Design and Performance of an Improved Trapped Vortex Combustor", Chinese Journal of Aeronautics, Vol. 25, No. 6, 2012, pp.864-870, https://doi.org/10.1016/S1000-9361(11)60456-1.

[8] R.C. Zhang, W.J. Fan, Q. Shi, W.L. Tan, "Combustion and emissions characteristics of dual-channel double-vortex combustion for gas turbine engines", Applied Energy, Vol. 130, 2014, pp.314-325, https://doi.org/10.1016/j.apenergy.2014.05.059.

[9] Ping Jiang, Xiaomin He, "Experimental investigation of flow field characteristics in a mixed-flow trapped vortex combustor", Aerospace Science and Technology, Vol. 96,2020, https://doi.org/10.1016/j.ast.2019.105533.

[10] P.K. Ezhil Kumar, D.P. Mishra, "Combustion noise characteristics of an experimental 2D trapped vortex combustor", Aerospace Science and Technology, Vol. 43, 2015, pp.388-394, https://doi.org/10.1016/j.ast.2015.03.014.

[11] Yuxi Guo, Cheng Gong, Yakun Huang, Fei Duan, Xiaomin He, "Combustion and emission performance of swirling-flow single trapped vortex combustor", Applied Thermal Engineering, Vol. 236,2024, https://doi.org/10.1016/j.applthermaleng. 2023.121678.

[12] R. Sharifzadeh, A. Afshari,"Assessment of a hydrogen-fueled swirling trapped-vortex combustor using large-eddy simulation", Fuel, Vol. 357, 2024, https://doi.org/10.1016/j.fuel. 2023.129847.

[13] Zheng, B., Zhang, Y. & Xie, J, "Investigation of performance in a cylindrical trapped vortex combustor with swirler", Heat Mass Transfer, Vol. 59, 2023, pp.1121–1137, https://doi.org/10.1007/s00231-022-03319-7

[14] Wensheng Zhao, Weijun Fan, Rongchun Zhang, "Study on the effect of fuel injection on combustion performance and NO_x emission of RQL trapped-vortex combustor", Energy Reports, Vol 9, No. 6, 2023, pp.54-63, https://doi.org/10.1016/j.egyr.2023.04.028.

[15] Anderson, W.S., Radtke, J.T., King, P.I., Thornburg, H., Zelina, J., Sekar, B., "Effects of Main Swirl Direction on High-g Combustion," 44th AIAA/ASME/SAE/ASEE Joint Propulsion Conference & Exhibit, 21-23 July 2008, Hartford, CT., AIAA2008-4954, 2008.

[16] Ali M. Jawarneh, M. Al-Widyan,A. Al-Migdady, H. Tlilan, M. Tarawneh, A. Ababneh, "Double vortex generators for increasing the separation efficiency of the air separator", International Journal of Heat and Technology (IJHT), Vol. 35, No. 3, 2017, pp. 529-538.

[17] Ali M. Jawarneh, "Investigation of the Flow Characteristics in a Sink-Swirl Flow within Two Disks", International Review of Mechanical Engineering, Vol. 7, No. 6, 2013, pp. 1031-1036.

[18] Ali M. Jawarneh, "Heat Transfer Enhancement in a Narrow Concentric Annulus in Decaying Swirl Flow", Heat Transfer Research, Vol. 42, No. 3, 2011, pp. 199-216.

[19] Ali M. Jawarneh, A. Al-Shyyab, H. Tlilan,A. Ababneh, "Enhancement of a cylindrical separator efficiency by using double vortex generators", Energy Conversion and Management, Vol. 50, No. 6, 2009, pp.1625-1633.

[20] Ali M. Jawarneh, H. Tlilan, A. Al-Shyyab, A. Ababneh, "Strongly Swirling Flows in a Cylindrical Separator", Minerals Engineering, Vol. 21, No. 5, 2008, pp. 366-372.

[21] Ali M. Jawarneh, G.H. Vatistas, "Reynolds Stress Model in the Prediction of Confined Turbulent Swirling Flows", Transaction of the ASME, Journal of Fluids Engineering, Vol. 128, No. 6, 2006, pp.1377-1382.

[22] Bouziane, A. Olivani, A. Khalfi, F. Cozzi, A. Coghe, "Experimental Investigation of Swirl-Stabilized Syngas Flames by Transverse Fuel Injection', Jordan Journal of Mechanical and Industrial Engineering, Vol. 2, No. 3, 2008, pp. 137-142.

[23] Ali M. Jawarneh, Georgios H. Vatistas, and Amer Ababneh, "Analytical Approximate Solution for Decaying Laminar Swirling Flows within A Narrow Annulus', Jordan Journal of Mechanical and Industrial Engineering, Vol. 2, No. 2, 2008, pp. 101 - 109.

[24] P.Vijayabalan and G. Nagarajan, "Performance, Emission and Combustion of LPG Diesel Dual Fuel Engine using Glow Plug", Jordan Journal of Mechanical and Industrial Engineering, Vol. 3, No. 2, 2009, pp. 105 - 110.

[25] K. Rajan and K. R. Senthilkumar, "Effect of Exhaust Gas Recirculation (EGR) on the Performance and Emission Characteristics of Diesel Engine with Sunflower Oil Methyl Ester", Jordan Journal of Mechanical and Industrial Engineering, Vol. 3, No. 4, 2009, pp. 306 - 311.

[26] Artem V.B., Shota A.P., and Alexander I.G., "Results of Numerical Modeling of Combustion Processes in a Vortex Chamber", ComPhysChem'18, MATEC Web of Conferences 209, 00023, 2018.

[27] Zejun Wu, Xiaomin He, Bo Jiang, Yi Jin., "Experimental investigation on a single cavity trapped vortex combustor", International Communications in Heat and Mass Transfer, Vol. 68, 2015, pp.8-13, doi.org/10.1016/j.icheatmasstransfer. 2015.08.003.

[28] Siva Kumara, D. Maheswarb, K. Vijaya Kumar Reddy, "Comparision of Diesel Engine Performance and Emissions from Neat and Transesterified Cotton Seed Oil", Jordan Journal of Mechanical and Industrial Engineering, Vol. 3, No. 3, 2009, pp. 190 – 197.

[29] Ajay V. Kolhe, R.E.Shelke and S.S.Khandare, "Performance and Combustion Characteristics of a DI Diesel Engine Fueled with Jatropha Methyl Esters and its Blends", Jordan Journal of Mechanical and Industrial Engineering, Vol. 8, No. 1, 2014, pp. 7-12.

[30] Rashid Ali, Anshumaan Singh, "Numerical Study of Fluid Dynamics and Heat Transfer Characteristics for the Flow Past a Heated Square Cylinder", h of Mechanical and Industrial Engineering, Vol. 15, No. 4, 2021, pp. 357 - 376.